Charged fluid nonconducting toroidal structures orbiting a Schwarzschild black hole immersed in a split-monopole magnetic field

Zdeněk Stuchlík,[*] Martin Blaschke,[†] Jiří Kovář,[‡] and Petr Slaný[§]

Research Centre for Theoretical Physics and Astrophysics, Institute of Physics, Silesian University in Opava, Bezručovo náměstí 13, CZ-746 01 Opava, Czech Republic

(Received 3 September 2021; accepted 30 March 2022; published 11 May 2022)

We study the existence of charged fluid nonconducting structures orbiting in the background given by a Schwarzschild black hole immersed in a monopolelike magnetic field introduced in the context of the Blandford-Znajek process. Due to fact that the split-monopole magnetic field is not defined in the equatorial plane, where typical accretion disks are located, we focus on searching for off-equatorial charged toroidal structures. We demonstrate that charged nonconducting tori can arise very close to the symmetry axis of the magnetized black hole; thus representing a possible obstacle for jets created due to the Blanford-Znajek process.

DOI: 10.1103/PhysRevD.105.103012

I. INTRODUCTION

The extraordinary energy outputs from quasars and active galactic nuclei with central supermassive black holes, or microquasars located in binary systems containing a stellar mass black hole, are caused by accretion disks orbiting the central black hole, and by the jets related to the disks. The accretion disk theory is very complex at its present state, as shown e.g., in [1], but it can be separated into two large classes; namely of the geometrically thin, Keplerian, accretion disks whose structure is mainly governed by the spacetime circular geodesics [2], and the geometrically thick, toroidal accretion disks governed by the effective potential of orbiting perfect fluid determined by the Euler equation, i.e., by the interplay of the gravitational and other inertial forces, and of the pressure gradients [3,4]. Closed equipotential surfaces of the effective potential determine equilibrium toroidal structures, while accretion (excretion) is related to self-crossing equipotential surfaces; open equipotential surfaces around the rotation axis govern jets. Complex equatorial tori orbiting Kerr black holes, reflecting simultaneous existence of relatively counter-rotating structures that could be created during the evolution of accretion structures in active galactic nuclei, were studied in [5–9].

For both Keplerian and toroidal accretion disks external magnetic fields could be very important [10]. They can substantially influence structure of ionized Keplerian disks, leading in the most extreme cases to their destruction [11–15]. In the external magnetic fields around black holes even off-equatorial charged-particle circular orbits are possible [16–18]. In complex magnetohydrodynamic approach [19,20], the fluid plasma structures are usually studied in the force-free approximation corresponding to infinite conductivity that was introduced for modeling of jets due to the so-called Blanford-Znajek process [21] (for recent comments on the relation of the Blandford-Znajek process and the magnetic Penrose process see [22,23]). Here we consider an opposite limit of zero conductivity for the so-called 'nonconducting (or dielectric) tori' introduced in [24] and further developed in [25–31]; such charged nonconducting tori can be equatorial, but can also be levitating outside the equatorial plane due to the electromagnetic interaction of the fluid charge with the magnetic field, thus creating complementary charged fluid structures to the equatorial ones. It is necessary to point out that in our scenario, in principle, we do not consider the nonconducting matter, in general, but the fluid consisting of free charged particles (i.e., a conducting fluid). However, when circling around the considered central black hole endowed with a magnetic field, the electric current is considered only because of the charge convection (the convection current by rotation of the fluid) and not because of a conduction; the charges are adherent to the circling charged particles or directly represent them. Thus, we assume the scenario where the "inertia" of circling particles dominates the "electromagnetic action" that is the opposite limit of the widely used limit of the fluid where the conduction current predominates—the limit of perfectly conducting (infinite conductivity) quasineutral fluid—plasma. Since the real fluid (accretion disks) rotating around compact objects endowed with (or immersed in) magnetic fields manifests with a certain finite conductivity, where the electric current is represented by both the convection and conduction currents, we believe

[*]zdenek.stuchlik@physics.slu.cz
[†]martin.blaschke@physics.slu.cz
[‡]jiri.kovar@physics.slu.cz
[§]petr.slany@physics.slu.cz

that the presented nonconducting limit is also very important to be surveyed as the direct opposite to the force-free infinite conductivity limit.

The exact shape and structure of the magnetic fields around black holes is still under examination, but the uniform magnetic field assumption introduced by Wald [32] can be used as an appropriate simple approximation to more complex fields. In the Kerr (Schwarzschild) black hole spacetimes and the uniform or dipole external magnetic fields, the charged nonconducting fluid structures were studied demonstrating that the equatorial tori give interesting complex structures from the astrophysical and observational point of view—they can constitute even doubled equatorial structures that can be accompanied by off-equatorial tori or clouds [25,27–30,33]; it has been shown that the off-equatorial tori having sufficiently low density can be considered as collisionless plasma [26].

In all the studies of the charged nonconducting fluid tori orbiting in the field of magnetized black holes the external magnetic field that can be completed by a Coulomb electric field was assumed to be asymptotically uniform, or of dipole character. However, there are some other possibilities of the magnetic field that are of astrophysical relevance. Here we consider the special case of split-monopole magnetic field that is considered in the first treatment of the Blandford-Znajek process [21] and later its relevance was confirmed for the magnetic fields generated by currents in thin accretion disks [20], or for magnetosphere by accretion configurations corresponding to the Blandford-Znajek process, restricted to vicinity of the black hole horizon [34]. Thus, we first introduce the model of the equilibrium or accretion charged fluid structures, and then discuss the tori in the field of Schwarzschild black hole with the split-monopole magnetic field that can be considered as a simple but realistic approximation for more realistic fields.

In the following, we use the geometric system of units, $c = G = k_{\rm B} = 1/4\pi\varepsilon_0 = 1$. Moreover, when considering our particular background fields, we also scale quantities by the spacetime mass parameter, M; thus, we use the dimensionless units there.

II. THE MODEL

The considered model of charged fluid toroidal configurations describes stationary and axisymmetric nonconducting equilibrium configurations of a perfect fluid with locally measured charge density q_ϱ, energy density ϵ, and pressure p profiles enabling their orbiting with the four-velocity field U^α in a fixed background gravitational, $g_{\alpha\beta}$, and electromagnetic, $F_{\alpha\beta} = \nabla_\alpha A_\beta - \nabla_\beta A_\alpha$, fields. The considered background fields must reflect simultaneous axial symmetry along with the symmetry of the orbiting fluid. The charged-fluid configurations are assumed to be test configurations from the general relativity point of view, being sufficiently low mass and weakly charged and thus having negligible influence on the background gravitational and external electromagnetic fields. The charged fluid configurations can be then determined by equations following from the general energy-momentum conservation law

$$\nabla_\beta \mathcal{T}^{\alpha\beta} = 0, \tag{1}$$

where the energy-momentum tensor $\mathcal{T}^{\alpha\beta} = T^{\alpha\beta} + T^{\alpha\beta}_{\rm em}$, with its parts

$$T^{\alpha\beta} = (\epsilon + p)U^\alpha U^\beta + p g^{\alpha\beta}, \tag{2}$$

$$T^{\alpha\beta}_{\rm em} = \frac{1}{4\pi}\left(\mathcal{F}^\alpha_{\ \gamma}\mathcal{F}^{\beta\gamma} - \frac{1}{4}\mathcal{F}_{\gamma\delta}\mathcal{F}^{\gamma\delta}g^{\alpha\beta}\right), \tag{3}$$

describes a charged fluid with negligible viscosity and heat conduction. The general electromagnetic part of this tensor is related to the Faraday tensor having two parts, $\mathcal{F}^{\alpha\beta} = F^{\alpha\beta} + F^{\alpha\beta}_{\rm self}$, where the background and the self-electromagnetic components satisfy the Maxwell equations

$$\nabla_\beta F^{\alpha\beta} = 0, \qquad \nabla_\beta F^{\alpha\beta}_{\rm self} = 4\pi J^\alpha, \tag{4}$$

with the four-current density field of the charged fluid J^α satisfying the linearized general Ohms law [35]

$$J^\alpha = q_\varrho U^\alpha + \sigma \mathcal{F}^{\alpha\beta}U_\beta \equiv j_{\rm v} + j_{\rm d}, \tag{5}$$

where $j_{\rm v}$ denotes the convection (inertial) current and $j_{\rm d}$ the conduction (electromagnetic) current. In the commonly accepted and applied approach in the so-called force-free models (see e.g., [21]), it is assumed that the conductivity $\sigma \to \infty$, and the dynamics of the charged matter is governed by the relation $\mathcal{F}^{\alpha\beta}U_\beta = 0$. In our approach of the nonconducting charged-fluid tori we abandon the second term in Ohms law, the conduction current $j_{\rm d}$, assuming $\sigma \to 0$. This approach reflects the assumption that the charges are fixed to the rotating matter. Moreover, we assume the electromagnetically test fluid, $F^{\alpha\beta}_{\rm self} \ll F^{\alpha\beta}$. Recall that the assumption of vanishing conductivity is necessary condition for the self-consistency of the axial symmetry of the model of charged fluid equilibrium configurations, as the nonzero conductivity implies due to the Ohm law existence of radial electric flows [36]—for details see [28]. Thus, we use the reduced form of Ohms law

$$J^\alpha = q_\varrho U^\alpha. \tag{6}$$

The assumption $\sigma \to 0$ and the following reduced form of Ohms law (6) is relevant for the scenario of a fluid consisting of elements (particles) possessing sufficiently small specific charge, $q = e/m = q_\varrho/\varrho$, where e is the

charge of the fluid elements, m is their mass or sufficiently small collision time, τ, moving in gravitational and sufficiently weak electromagnetic fields. This is because for $|Be\tau/m| \ll 1$, where $B_\alpha = \frac{1}{2}\epsilon_{\alpha\beta\gamma\delta}F^{\gamma\delta}U^\beta$, the conductivity can be determined as $\sigma = n_e e^2\tau/m$, where $n_e = q_\varrho/e$ is the fluid element density [37]. Thus, in this case, the generalized Ohms law (5) can be written in the form $J^\alpha = q_\varrho U^\alpha + q_\varrho(e\tau/m)F^\alpha{}_\beta U^\beta$. Then, for $|e\tau/m| \ll 1$ and for weak electromagnetic fields, i.e., for small magnitudes of components of $F^\alpha{}_\beta = g^{\alpha\gamma}F_{\gamma\beta}$ (as compared to unity), we find $q_\varrho(e\tau/m)F^\alpha{}_\beta U^\beta \ll q_\varrho U^\alpha$. Thus, $j_{\rm d} \ll j_{\rm v}$, and consequently $J^\alpha \approx q_\varrho U^\alpha$. As an example of such a scenario, we can mention free protons in a massive neutron star interior forming a charged ideal superfluid flowing by itself and interacting only with the gravitational and electromagnetic fields [37].

A. Balance equations of the fluid

Basic features of the charged fluid model of toroidal configurations can be summarized as follows: The elementary charges in the fluid are adherent to the fluid elements, i.e., we assume $\sigma \to 0$; the charged elements are uniformly rotating in the azimuthal direction with the four-velocity field $U^\alpha = (U^t, 0, 0, U^\varphi)$ and $U^\alpha \neq U^\alpha(t, \varphi)$. Presuming the electromagnetically test fluid, $F^{\alpha\beta}_{\rm self} \ll F^{\alpha\beta}$, the general energy-momentum conservation law (1) reduces to the form of the equation of motion [24]

$$\nabla_\beta T^{\alpha\beta} = F^{\alpha\beta}J_\beta, \tag{7}$$

governing the orbiting charged fluid. The related fluid-flow pressure balance equations take the form

$$\begin{aligned}\partial_r p &= -(p+\epsilon)\mathbb{R}^\circ + q_\varrho \mathbb{R}^* \equiv \mathbb{R},\\ \partial_\theta p &= -(p+\epsilon)\mathbb{T}^\circ + q_\varrho \mathbb{T}^* \equiv \mathbb{T}.\end{aligned} \tag{8}$$

We denote the right-hand sides of these equations governing the pressure gradients guaranteeing the fluid balance as $\mathbb{R} = \mathbb{R}(r,\theta)$ and $\mathbb{T} = \mathbb{T}(r,\theta)$, separating them into two parts—the purely hydrodynamical, and the additional magnetohydrodynamical that are given by the relations

$$\begin{aligned}\mathbb{R}^\circ &= \partial_r \ln|U_t| - \frac{\Omega\partial_r\ell}{1-\Omega\ell}, \qquad \mathbb{R}^* = U^t\partial_r A_t + U^\varphi\partial_r A_\varphi,\\ \mathbb{T}^\circ &= \partial_\theta \ln|U_t| - \frac{\Omega\partial_\theta\ell}{1-\Omega\ell}, \qquad \mathbb{T}^* = U^t\partial_\theta A_t + U^\varphi\partial_\theta A_\varphi.\end{aligned}$$

The standard fluid models of toroidal configurations [3] are governed by the pure hydrodynamic parts $\mathbb{R}^\circ$ and $\mathbb{T}^\circ$.

The specific angular momentum profile of the rotating fluid, $\ell = -U_\varphi/U_t$, and the angular velocity related to the static distant observers, $\Omega = U^\varphi/U^t$, are related by the formula

$$\Omega = -\frac{\ell g_{tt} + g_{t\varphi}}{\ell g_{t\varphi} + g_{\varphi\varphi}}, \tag{9}$$

and the profile of the time component of the four-velocity U_t is related to the specific angular momentum profile as

$$(U_t)^2 = \frac{g_{t\varphi}^2 - g_{tt}g_{\varphi\varphi}}{\ell^2 g_{tt} + 2\ell g_{t\varphi} + g_{\varphi\varphi}}. \tag{10}$$

The axial component of the four-velocity field is then given by the relation $U_\varphi = -\ell U_t$. Derivation of the pressure Eqs. (8) can be found in [24,27,28]; their uncharged limit $q_\varrho = 0$ corresponds to the Euler equation describing a rotating electrically neutral perfect fluid [3,38–40].

Note that since we consider $q_\varrho = q_\varrho(r,\theta)$, $U^t = U^t(r,\theta)$, $U^\varphi = U^\varphi(r,\theta)$, $U^\alpha = (U^t, 0, 0, U^\varphi)$ in our model, then for the considered four-current density (6) we have $\nabla_\alpha J^\alpha = U^\alpha\partial_\alpha q_\varrho + q_\varrho\nabla_\alpha U^\alpha = q_\varrho\frac{1}{\sqrt{-g}}(\sqrt{-g}\partial_\alpha U^\alpha) = 0$, i.e., the four-current density is conserved.

1. Rotation regime and charge distribution

In general, all solutions $p(r,\theta)$ of the set of equations (8) are subjected to the integrability condition

$$\partial_\theta\mathbb{R} = \partial_r\mathbb{T}, \tag{11}$$

which must be assumed simultaneously. Thus, the profiles of the specific angular momentum $\ell = \ell(r,\theta)$ [angular velocity $\Omega = \Omega(r,\theta)$] and the charge density $q_\varrho = q_\varrho(r,\theta)$ must be properly adjusted to each other in accord with this integrability condition. To close the system of equations, we assume perfect fluid with the polytropic energy density and pressure relations

$$p = \kappa\varrho^\Gamma, \qquad \epsilon = \varrho + \frac{1}{\Gamma-1}p, \tag{12}$$

with κ and Γ being the polytropic coefficient and exponent.

2. Analytic solution of the balance equations

An analytic integration of the balance pressure equations leading to a particular class of solutions is based on an introduction of the charge density transformation formula

$$\mathcal{K} = \frac{q_\varrho}{\epsilon + p}U^\varphi, \tag{13}$$

and the pressure transformation relations

$$\partial_r w = \frac{\partial_r p}{(p+\epsilon)}, \qquad \partial_\theta w = \frac{\partial_\theta p}{(p+\epsilon)}, \tag{14}$$

whereas in the considered case $A_\alpha = (0,0,0,A_\varphi)$, we arrive at the transformed pressure balance equations

$$\partial_r w = -\partial_r \ln|U_t| + \frac{\Omega\partial_r \ell}{1-\Omega\ell} + \mathcal{K}\partial_r A_\varphi,$$
$$\partial_\theta w = -\partial_\theta \ln|U_t| + \frac{\Omega\partial_\theta \ell}{1-\Omega\ell} + \mathcal{K}\partial_\theta A_\varphi. \quad (15)$$

Due to the considered axial symmetry, where there are $U^t = U^t(r,\theta)$, $U^\varphi = U^\varphi(r,\theta)$, $\ell = -U_\varphi/U_t = \ell(r,\theta)$, and $A_\varphi = A_\varphi(r,\theta)$, the related differentials can be written in the form

$$\mathrm{d}A_\varphi = \partial_r A_\varphi \mathrm{d}r + \partial_\theta A_\varphi \mathrm{d}\theta, \quad (16)$$

$$\mathrm{d}\ell = \partial_r \ell \mathrm{d}r + \partial_\theta \ell \mathrm{d}\theta, \quad (17)$$

$$\mathrm{d}\ln|U_t| = \partial_r \ln|U_t|\mathrm{d}r + \partial_\theta \ln|U_t|\mathrm{d}\theta. \quad (18)$$

The differentials can be incorporated into the system of Eqs. (15) (multiplied by $\mathrm{d}r$ and $\mathrm{d}\theta$), which yields the Pfaffian form

$$\mathrm{d}w = -\mathrm{d}\ln|U_t| + \frac{\Omega}{1-\Omega\ell}\mathrm{d}\ell + \mathcal{K}\mathrm{d}A_\varphi, \quad (19)$$

that can be easily integrated as

$$\int_0^w \mathrm{d}w = -\ln\left|\frac{U_t}{U_{t_{\mathrm{in}}}}\right| + \int_{\ell_{\mathrm{in}}}^{\ell} \frac{\Omega\mathrm{d}\ell}{1-\Omega\ell} + \int_{A_{\varphi\mathrm{in}}}^{A_\varphi} \mathcal{K}\mathrm{d}A_\varphi, \quad (20)$$

if $\Omega = \Omega(\ell)$ and $\mathcal{K} = \mathcal{K}(A_\varphi)$. Then, the solution of the set of Eqs. (15) can be written in the form

$$w = \int_0^w \mathrm{d}w = -W + W_{\mathrm{in}}. \quad (21)$$

The function $W(r,\theta)$ denotes an effective potential variable part of the right-hand side of Eq. (20), and the subscript 'in' relates to the position of a particular inner edge of the orbiting fluid structure at $r = r_{\mathrm{in}}$ for $\theta = \theta_{\mathrm{in}}$, whereas for a function $X = X(r,\theta)$, we denote $X_{\mathrm{in}} = X(r_{\mathrm{in}},\theta_{\mathrm{in}})$. Moreover, W_{in} plays the role of a constant of integration.

The pressure transformation relations (14) are integrated so that

$$\int_0^w \mathrm{d}w = \int_0^p \frac{\mathrm{d}p}{p+\epsilon}, \quad (22)$$

if we consider a barotropic fluid, i.e., $\epsilon = \epsilon(p)$, guaranteed by the chosen polytropic equation of state (12). The equipressure surfaces, $p = \mathrm{const.}$, determining the topology of the orbiting fluid structure, are of the same shape as the equipotential surfaces, $W = \mathrm{const}$. The effective potential fully governs behavior of the stationary and axisymmetric fluid configurations both for uncharged fluids [38,40] and for considered charged fluids [27,28] as well.

Note that the employed conditions $\Omega = \Omega(\ell)$ and $\mathcal{K} = \mathcal{K}(A_\varphi)$ guarantee the integrability of the system of Eqs. (15), as we can also easily see after checking the integrability condition (11) that reads

$$\partial_\theta(f\partial_r\ell + \mathcal{K}\partial_r A_\varphi) = \partial_r(f\partial_\theta\ell + \mathcal{K}\partial_\theta A_\varphi). \quad (23)$$

Here, we denote $f = \Omega/(1-\Omega\ell)$, and since we assume $\Omega = \Omega(\ell)$ and $\mathcal{K} = \mathcal{K}(A_\varphi)$, then $\partial_\theta f = \partial_\ell f \partial_\theta \ell$, $\partial_r f = \partial_\ell f \partial_r \ell$, $\partial_\theta \mathcal{K} = \partial_{A_\varphi}\mathcal{K}\partial_\theta A_\varphi$, $\partial_r \mathcal{K} = \partial_{A_\varphi}\mathcal{K}\partial_r A_\varphi$, thus the integrability condition is satisfied.

III. BLACK HOLE WITH SPLIT-MONOPOLE MAGNETIC FIELD

In the following section, we focus on the charged nonconducting fluid structures rotating around the Schwarzschild black hole with its spacetime geometry line element

$$\mathrm{d}s^2 = g_{tt}\mathrm{d}t^2 + g_{rr}\mathrm{d}r^2 + g_{\theta\theta}\mathrm{d}\theta^2 + g_{\varphi\varphi}\mathrm{d}\varphi^2, \quad (24)$$

where

$$g_{\theta\theta} = r^2, \qquad g_{\varphi\varphi} = r^2\sin\theta^2,$$
$$g_{tt} = -f(r), \qquad g_{rr} = f(r)^{-1}, \quad (25)$$

and $f(r) = 1\text{–}2/r$, immersed in a split-monopole test magnetic field described by the four-vector electromagnetic potential [21]

$$A_\alpha = (0,0,0,g|\cos\theta|), \quad (26)$$

with the parameter g governing the strength of the magnetic field. Note that the split-monopole magnetic field shares with the spacetime its symmetries, i.e., it is static and spherically symmetric.

Since no magnetic monopole solutions are assumed in the electrodynamics, i.e., the magnetic field B^a must satisfy the condition $\nabla_a B^a = 0$, the considered monopole solution is the split one with an imaginary source in the origin, and with the orientation of the magnetic field lines inversed below the equatorial plane—the forbidden region (see Fig. 1.); in the following, we consider only the part above the equatorial plane, $0 \le \theta < \pi/2$.

The split-monopole magnetic field was introduced for modeling of creation of jets in magnetospheres of rotating black holes in regions close to their horizons [21]. The physical relevance of this special kind of magnetic field was confirmed by numerical models of magnetohydrodynamic processes around black holes [20], where it was demonstrated that the source of such a magnetic field can be an electric flow in a thin equatorial accretion disk, or that such a field can appear in a vicinity of black hole or

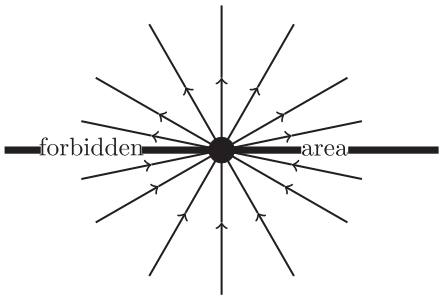

FIG. 1. Scheme of a split-monopole magnetic field.

magnetosphere giving rise to the Blandford-Znajek process of jet acceleration [34].

The split-monopole magnetic field can be well characterized by a local observer tetrad three-vector field $B_{(a)}$ with the only nonvanishing component

$$B_{(r)} = F_{(\varphi\theta)} = e^{\varphi}_{(\varphi)} e^{\theta}_{(\theta)} F_{\varphi\theta}, \tag{27}$$

being transformed to the Schwarzschild coordinate basis as

$$B_r = \frac{e^{\varphi}_{(\varphi)} e^{\theta}_{(\theta)}}{e^{r}_{(r)}} F_{\varphi\theta}, \tag{28}$$

where $e^{r}_{(r)} = g_{rr}^{-1/2}$, $e^{\varphi}_{(\varphi)} = g_{\varphi\varphi}^{-1/2}$ and $e^{\theta}_{(\theta)} = g_{\theta\theta}^{-1/2}$ are the nonvanishing components of the tetrad basis vectors $e^{\alpha}_{(r)}$, $e^{\alpha}_{(\varphi)}$, and $e^{\alpha}_{(\theta)}$.

In the considered background, and thanks to the expression $F_{\alpha\beta} = \nabla_\alpha A_\beta - \nabla_\beta A_\alpha$, there is also only a radial contravariant nonvanishing vector-field component

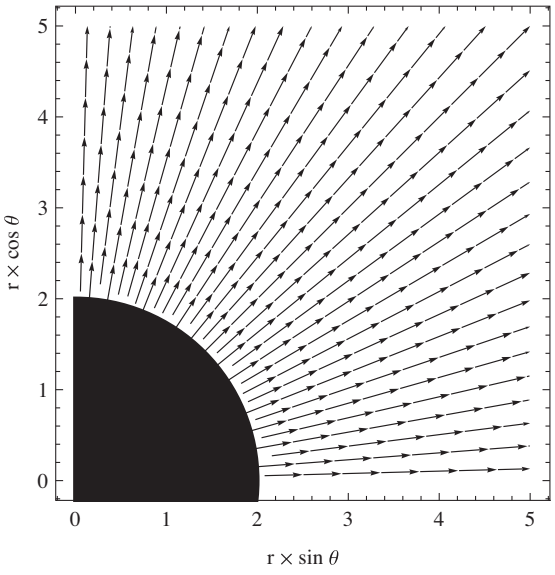

FIG. 2. Split-monopole magnetic field lines determined by their tangent vector field B^a.

$$B^r = -e^{r}_{(r)} e^{\varphi}_{(\varphi)} e^{\theta}_{(\theta)} \partial_\theta A_\varphi, \tag{29}$$

thus fully satisfactory for the magnetic field visualization (see Fig. 2).

The strength of the magnetic field measured by local observers, $\mathcal{B} = (B^{(a)} B_{(a)})^{1/2}$, can be expressed as

$$\mathcal{B} = |e^{\varphi}_{(\varphi)} e^{\theta}_{(\theta)} \partial_\theta A_\varphi| = \frac{|g \sin\theta|}{(g_{\varphi\varphi} g_{\theta\theta})^{1/2}}. \tag{30}$$

Thus, it is related to the parameter g by the simple formula $|g| = \mathcal{B} r^2$. For those interested in the above mentioned astrophysical contextualization, we can note that in the case of, e.g., central Schwarzschild mass $M_{\rm SI} = 10^{10}\ \mathrm{M}_\odot$ and the magnetic field strength $\mathcal{B}_{\rm SI} = 10$ T measured at the dimensionless radius $r = 10$, the dimensionless parameter $g \approx 5 \times 10^{-3}$.

IV. OFF-EQUATORIAL TORI

Off-equatorial toroidal structures (tori) are the toroidal structures with their pressure maxima (centers) located above, or under, the equatorial plane of the considered background. Here, in the case of the Schwarzschild spacetime accompanied by the split-monopole magnetic field, there are $U^t = g^{tt} U_t$, $U^\varphi = g^{\varphi\varphi} U_\varphi$ and

$$(U_t)^2 = -\frac{f(r) r^2 \sin^2\theta}{\ell^2 f(r) - r^2 \sin^2\theta}. \tag{31}$$

The condition $(U_t)^2 > 0$ requires $\ell^2 f(r) - r^2 \sin^2\theta < 0$, implying the restriction on the acceptable values of the specific angular momentum in the form

$$\ell^2 < \frac{r^3 \sin^2\theta}{r-2} \equiv l^2_{\rm ph}(r,\theta). \tag{32}$$

Note that the function $l^2_{\rm ph}(r;\theta = \pi/2)$ governs the motion of photons in the equatorial plane, and for $l^2 = 27$ we obtain the circular photon orbit at $r = 3$ giving the innermost limit on position of circular geodesics.

Due to the simple form of the vector potential (26), the transformed pressure balance Eqs. (15) reduce to the form

$$\begin{aligned} \partial_r w &= -\partial_r \ln|U_t| + \frac{\Omega \partial_r \ell}{1 - \Omega\ell}, \\ \partial_\theta w &= -\partial_\theta \ln|U_t| + \frac{\Omega \partial_\theta \ell}{1 - \Omega\ell} + g\mathcal{K}\partial_\theta \cos\theta, \end{aligned} \tag{33}$$

whereas we require $\Omega = \Omega(\ell)$ and $\mathcal{K} = \mathcal{K}(\cos\theta)$ for the integrability to be satisfied. Thus, the solution can be written in the form

$$w = -\ln\left|\frac{U_t}{U_{t_{\rm in}}}\right| + \int_{\ell_{\rm in}}^{\ell}\frac{\Omega \mathrm{d}\ell}{1-\Omega\ell} + g\int_{\cos\theta_{\rm in}}^{\cos\theta}\mathcal{K}\mathrm{d}(\cos\theta) = -W + W_{\rm in}. \quad (34)$$

Below we demonstrate the existence of the off-equatorial tori with their centers, possibly located at $(r_{\rm c},\theta_{\rm c})$, corresponding to local minima of the effective potential W (maxima of the pressure p). Thus, these locations must satisfy the necessary conditions

$$\partial_r W|_{\substack{r=r_{\rm c}\\ \theta=\theta_{\rm c}}} = 0, \qquad \partial_\theta W|_{\substack{r=r_{\rm c}\\ \theta=\theta_{\rm c}}} = 0, \quad (35)$$

and, moreover, the sufficient conditions

$$\partial^2_{\theta\theta} W|_{\substack{r=r_{\rm c}\\ \theta=\theta_{\rm c}}} > 0, \qquad \det\mathcal{H}|_{\substack{r=r_{\rm c}\\ \theta=\theta_{\rm c}}} > 0, \quad (36)$$

where

$$\mathcal{H} = \begin{pmatrix} \partial^2_{rr}W & \partial^2_{r\theta}W \\ \partial^2_{\theta r}W & \partial^2_{\theta\theta}W \end{pmatrix}, \quad (37)$$

is the Hessian matrix. We survey a couple of rotation regimes of the fluid, particularly the case $\ell = \text{const.}$ and two cases $\ell \neq \text{const.}$ satisfying the condition $\Omega = \Omega(\ell)$, and the distribution of the charge density given by the monomial profile of the function $\mathcal{K} = \mathcal{K}(\cos\theta)$,

$$\mathcal{K} = \cos^{n-1}\theta, \quad (38)$$

integrated as $\int \mathcal{K}\mathrm{d}\cos\theta = \cos^n\theta/n$ for $n \neq 0$, and $\int \mathcal{K}\mathrm{d}\cos\theta = \ln|\cos\theta|$ for $n = 0$, relaxing the integration constants.

A. Rotation regime $\ell = \text{const}$.

The rotational regime $\ell = \text{const.}$ is an unique one, representing the marginally stable distribution of ℓ that is able to govern the basic properties of generally acceptable equilibrium tori [1]. In this case, the potential (34), governing the toroidal configurations, takes under our assumption $\mathcal{K} = \mathcal{K}(\cos\theta)$ the form

$$W = \ln|U_t| - g\int \mathcal{K}\mathrm{d}(\cos\theta), \quad (39)$$

where we neglect the integration constant.

The necessary conditions (35) implying the set of equations

$$\frac{r_{\rm c}\sin^2\theta_{\rm c} - \ell^2 f_{\rm c}^2}{f_{\rm c} r_{\rm c}(r_{\rm c}^2\sin^2\theta_{\rm c} - \ell^2 f_{\rm c})} = 0, \quad (40)$$

$$g\mathcal{K}_{\rm c}\sin\theta_{\rm c} - \frac{\ell^2 f_{\rm c}\cot\theta_{\rm c}}{r_{\rm c}^2\sin^2\theta_{\rm c} - \ell^2 f_{\rm c}} = 0, \quad (41)$$

relate values of the constants ℓ and g with the possible location of centers so that

$$g = \frac{\cot\theta_{\rm c}}{(r_{\rm c}-3)\sin\theta_{\rm c}\mathcal{K}_{\rm c}}, \quad (42)$$

$$\ell^2 = \frac{r_{\rm c}\sin^2\theta_{\rm c}}{f_{\rm c}^2}, \quad (43)$$

where $f_c \equiv f(r_c)$ and $\mathcal{K}_{\rm c} \equiv \mathcal{K}(\cos\theta_{\rm c})$. For the considered monomial form of the function $\mathcal{K}$ (38), the sufficient conditions (36) can be explicitly written as

$$\frac{(36-14r_{\rm c})\cos^2\theta_{\rm c} + (18-9r_{\rm c}+r_{\rm c}^2)(2-n)\sin^2\theta_{\rm c}}{r_{\rm c}^2(r_{\rm c}-3)^3(r_{\rm c}-2)\sin^2\theta_{\rm c}} > 0,$$
$$\frac{(4r_{\rm c}-10)\cos^2\theta_{\rm c} + (r_{\rm c}-3)(2-n)\sin^2\theta_{\rm c}}{(r_{\rm c}-3)^2\sin^2\theta_{\rm c}} > 0, \quad (44)$$

determining the region of existence of the potential W minima in the plane (r,θ) (see Fig. 3). Note that for a presentation of this region and for a presentation of profiles of W, it is more convenient to use the cylindrical coordinates

$$R = r\sin\theta, \qquad Z = r\cos\theta. \quad (45)$$

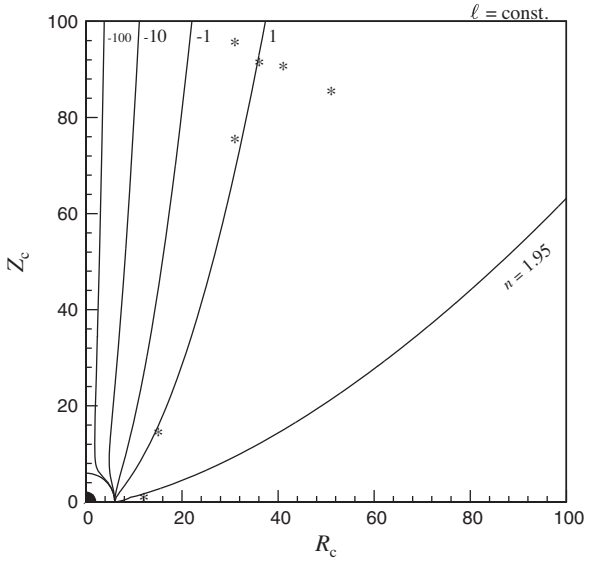

FIG. 3. Existence of minima of the potential W—centers of toroidal structures rotating with the specific angular-momentum profile $\ell = \text{const.}$ and with the monomial charge density distribution function $\mathcal{K} = \cos^{n-1}\theta$, for different values of the exponent n; for a chosen n, the minima exist in the region 'on the right' of the corresponding curve. The asterisks denote the positions of the potential minima shown in Figs. 5 and 6.

As it is clearly seen from the mentioned conditions, a position of potential minimum with the radius r_c and latitude θ_c is determined by values of the parameters ℓ, g, and n. To demonstrate corresponding mutual relations between these parameters and coordinates, we illustrate combinations of values of the parameters ℓ, g, and latitude θ_c allowing for formations of the potential minimum at a chosen radius r_c, for a fixed value of n (see Fig. 4). This figure fully represents the dependence of the minimum of the effective potential corresponding to the torus center on the parameters of the nonconducting charged configuration located off the equatorial plane. There is a clear observable tendency for torus center to be located closer to the symmetry axis ($\theta_c \sim 0$) because of decreasing value of the specific angular momentum ℓ, and charge distribution parameter n decreasing to negative values. As expected, shifting to large values of the parameter ℓ corresponds to the shifting of the center closer to the equatorial plane. Of course, Fig. 4 gives no information on the possible extension and shape of the nonconducting charged tori.

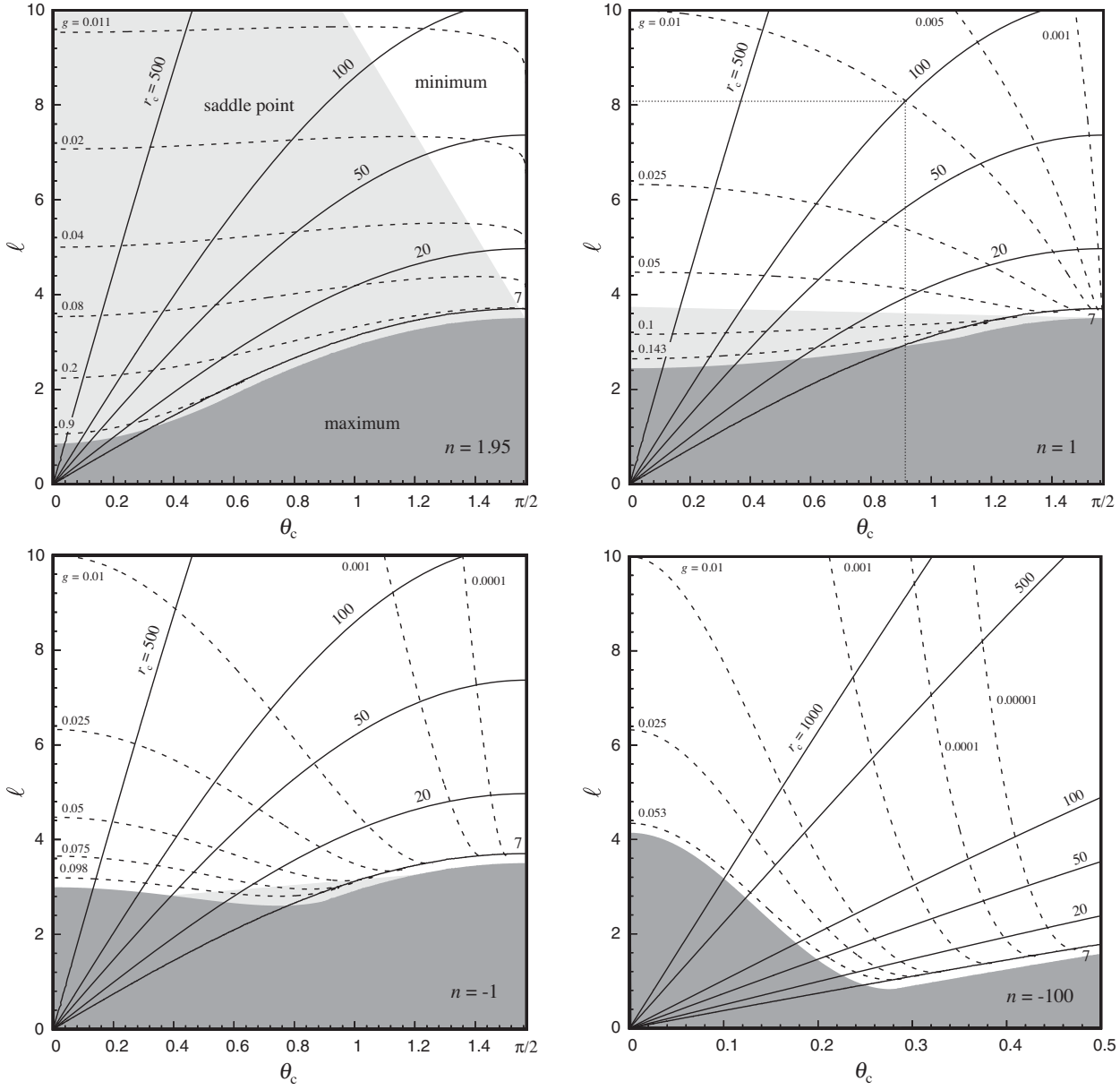

FIG. 4. Latitudes θ_c, angular momenta ℓ, and magnetic parameters g determining effective potential W minima with chosen radii $r_c \in \{500, 100, 50, 20, 7\}$, for fixed values of $n \in \{1.95, 1, -1, -100\}$. The figure can be read, e.g., in the following way. For the fixed value of $n = 1$ (top right part of the figure), the minimum at the radius $r_c = 100$ is formed at the latitude $\theta_c \doteq 0.92$ if the fluid rotates with the angular momentum $\ell \doteq 8.1$, in the magnetic field with its parameter $g = 0.01$. Note that while the white regions allow us to read positions of the studied minima of the effective potential W and related quantities, the light gray regions map saddle points, and the dark regions map maxima of the effective potential.

Behavior of the equipotential surfaces governing the extension and shape of the toroidal configurations is represented in Figs 5 and 6, where we fix the magnitude of the specific angular momentum l and the magnetic field parameter g in one case, and the charge distribution parameter n and the radius of the torus center r_c in the other one. We can see that very narrow and prolonged toroidal configurations usually occur as the symmetry axis is approached.

B. Rotation regime $\ell \neq$ const.

In the case of the rotational regime $\ell \neq$ const., the potential (34) takes the general form

$$W = \ln|U_t| - \int \frac{\Omega \mathrm{d}\ell}{1-\Omega\ell} - g\int \mathcal{K}\mathrm{d}(\cos\theta), \quad (46)$$

where we neglect the integration constants. Here the relation $\Omega = \Omega(\ell)$ required for the integrability is chosen so that

$$\Omega = \frac{\ell^{1+1/m}}{K^{1/m}}, \quad (47)$$

implying the specific angular momentum in the form

$$\ell = K\frac{f(r)^m}{r^{2m}\sin^{2m}\theta}, \quad (48)$$

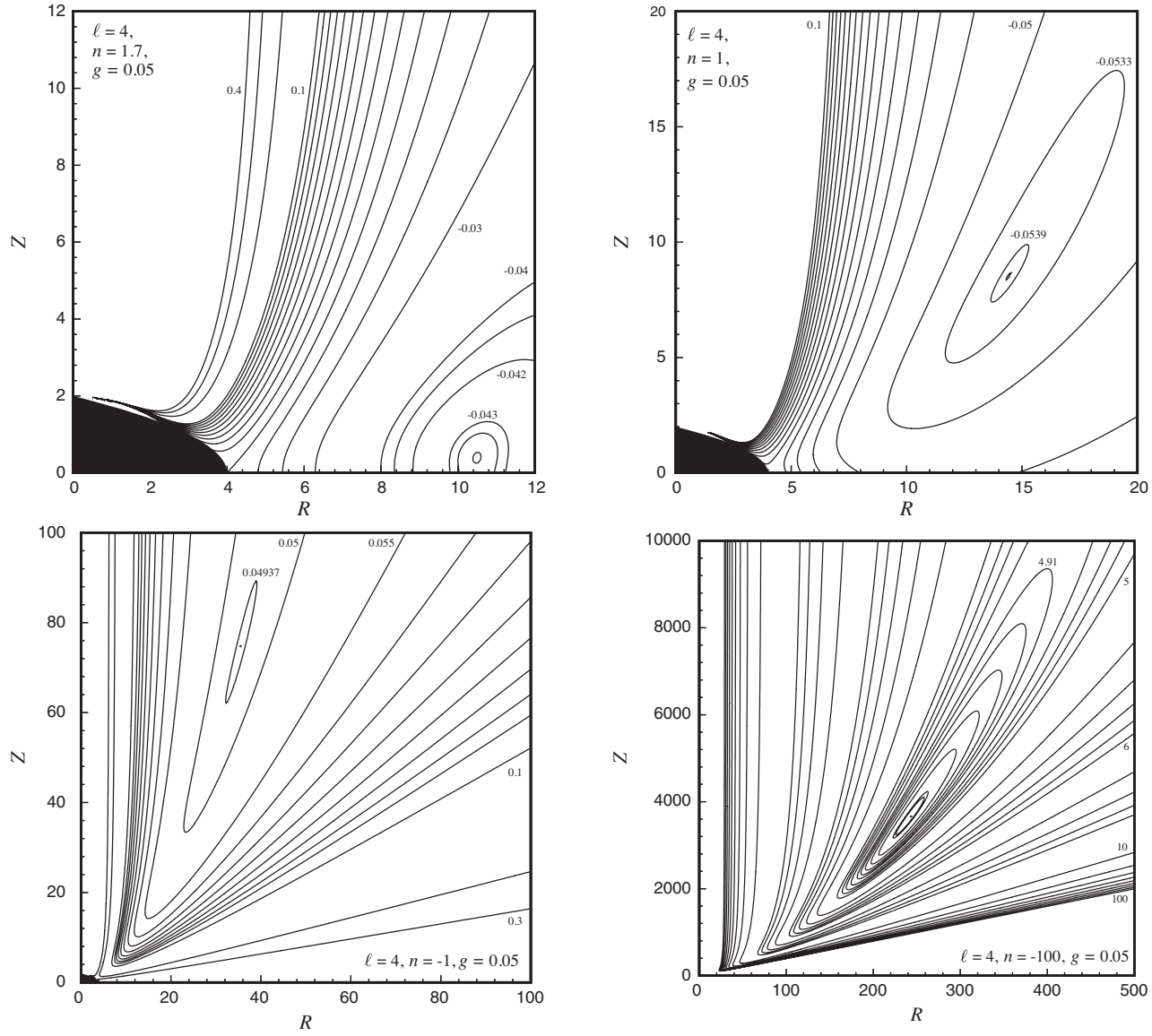

FIG. 5. Profiles of the potential W shown in terms of its poloidal contours corresponding to the fluid rotating with the specific angular momentum profile $\ell = 4$ and the monomial charge density distribution function $\mathcal{K} = \cos^{n-1}\theta$ with $n \in \{1.7, 1, -1, -100\}$, in the split-monopole magnetic field determined by the parameter $g = 0.05$.

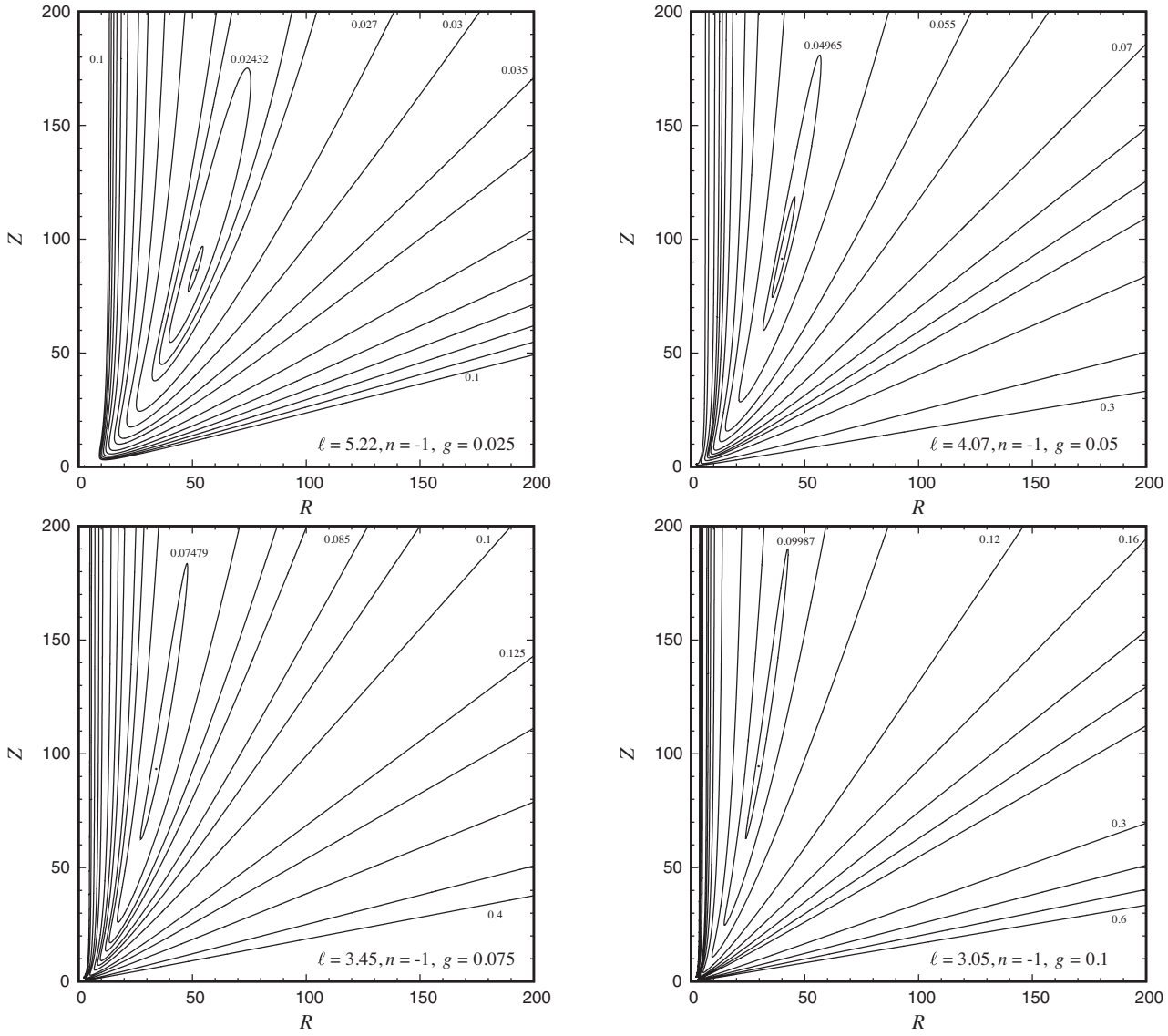

FIG. 6. Profiles of the potential W shown in terms of its poloidal contours corresponding to the fluid rotating with the specific angular momenta profiles $\ell \in \{5.22, 4.07, 3.45, 3.05\}$ and the monomial charge-density distribution function $\mathcal{K} = \cos^{n-1}\theta$ with $n = -1$, in the split-monopole magnetic field determined by the parameters $g \in \{0.025, 0.05, 0.075, 0.1\}$. The minima of the potential are located at the radius $r_c = 100$ in all the cases.

since Ω and ℓ are related to each other by the general formula (9) taking in the Schwarzschild spacetime the form

$$\Omega = \ell \frac{f(r)}{r^2 \sin^2\theta}. \tag{49}$$

1. Case $m = -1$

The case $m = -1$ corresponds to a rigid rotation of the fluid, $\Omega = K$, whereas the rotational part of the potential (46) takes the form

$$\int \frac{\Omega \mathrm{d}\ell}{1 - \Omega\ell} = -\ln\left|1 - \frac{\Omega^2 r^2 \sin^2\theta}{f(r)}\right|. \tag{50}$$

Due to the necessary conditions (35), in the centers of the toroidal structures, the constants g and Ω must take values

$$g = \frac{\cot\theta_c}{(r_c - 3)\sin\theta_c \mathcal{K}_c}, \tag{51}$$

$$\Omega^2 = \frac{1}{r_c^3 \sin^2\theta_c}. \tag{52}$$

Moreover, here, the sufficient conditions (36)

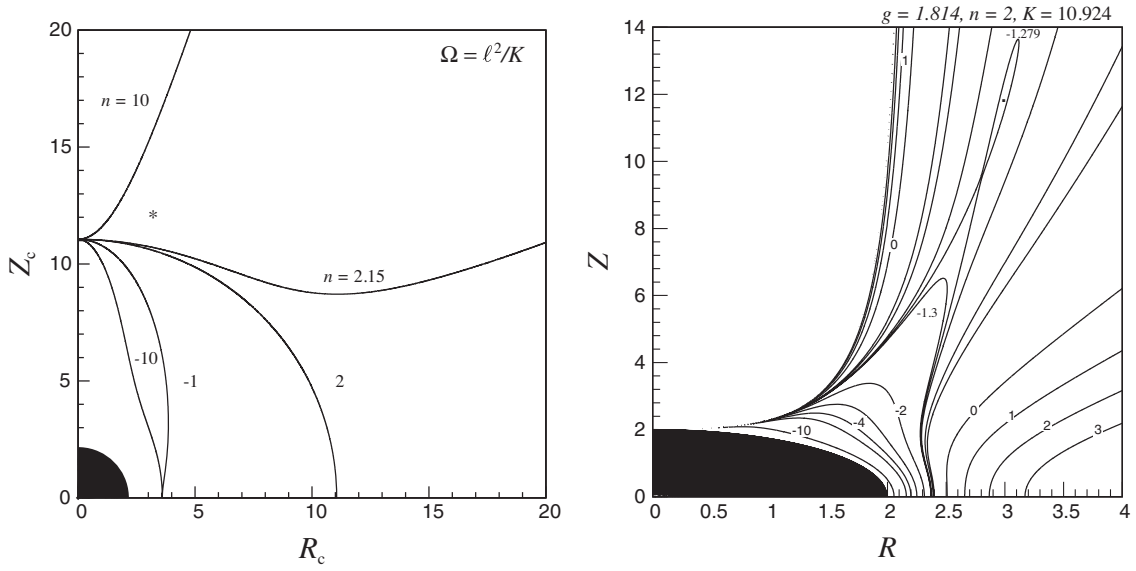

FIG. 7. Left: Existence of the minima of the potential W—centers of toroidal structures rotating with the angular velocity profile $\Omega = \ell^2/K$ and with the monomial charge density distribution function $\mathcal{K} = \cos^{n-1}\theta$, for different values of the exponent n; for a chosen value of n, the minima exist in the region 'above' the corresponding curve. The asterisk denotes position of the potential minimum shown in the right part of the figure. Right: Profile of the potential W shown in terms of its poloidal contours corresponding to the fluid rotating with $\Omega = \ell^2/K$, where $K = 10.924$, and the monomial charge density distribution function with $n = 2$, in the split-monopole magnetic field determined by the parameter $g = 1.814$.

$$\frac{3n(r_c-3)-2r_c+(18-4r_c)\cot^2\theta_c}{(r_c-3)^3 r_c^2} > 0$$
$$\frac{(2-n)(r_c-3)-2\cot^2\theta_c}{(r_c-3)^2} > 0, \quad (53)$$

must be satisfied. However, for any values of n of the considered monomial profile of the function $\mathcal{K}$ (38), there are no possible centers of the toroidal structures. Therefore, no rigidly rotating nonconducting charged toroidal configurations are allowed in the field of the split monopole.

2. Case $m = 1$

The case $m = 1$ corresponds to a rotation of the fluid with the angular velocity profile

$$\Omega = \frac{\ell^2}{K} = K\frac{f(r)^2}{r^4\sin^4\theta}, \quad (54)$$

whereas the corresponding rotational term of the potential (46) takes the form

$$\int \frac{\Omega \mathrm{d}\ell}{1-\Omega\ell} = -\frac{1}{3}\ln\left|1-\frac{K^2 f(r)^3}{r^6\sin^6\theta}\right|. \quad (55)$$

Due to the necessary conditions (35), in the centers of the toroidal structures, the constants g and K must take values

$$g = \frac{\cot\theta_c}{(r_c-3)\sin\theta_c \mathcal{K}_c}, \quad (56)$$

$$K = \pm\frac{r_c^3\sin^3\theta_c}{\sqrt{f_c^3(r_c-2)}}. \quad (57)$$

Moreover, here, the sufficient conditions (36)

$$\frac{6(r_c-2)r_c - n(r_c-3)(5r_c-18) + \frac{2(54+r_c(2r_c-27))}{\sin^2\theta_c}}{(r_c-3)^3(r_c-2)r_c^2} > 0,$$
$$\frac{3(4+n)-(6+n)r_c+\frac{2(4r_c-9)}{\sin^2\theta_c}}{(r_c-3)^2} > 0, \quad (58)$$

must be satisfied—see Fig. 7 where the allowed positions of the tori center are demonstrated along with an example of the equilibrium configurations allowed in vicinity of the symmetry axis. From the presented results we can conclude that the model is rich enough to support the off-equatorial nonconducting charged structures with the assumed special profile of the angular velocity. We again demonstrate that such off-equatorial tori located near the symmetry axis should be very narrow and prolonged, similarly to the case of the $\ell = \text{const.}$ configurations.

V. CONCLUSIONS

The Blandford-Znajek process is related to large acceleration of electrons and assumes force-free approximation of the electromagnetic processes where the inertial effects corresponding to the rest mass of accelerated particles can be fully abandoned—in the force-free approximation we thus consider matter with infinite conductivity. However,

around the magnetized black holes can be also much heavier particles (protons, heavy ions, or even dust particles), and in some circumstances (for properly chosen astrophysically relevant magnetic field intensity) their rest mass cannot be considered as negligible, implying irrelevance of the force-free approximation for these particles. In such a case we have to model the influence of electromagnetic field on the charged particles in different way, taking into account the rest mass of particles. For these purposes, the opposite approach based on the assumption of vanishing conductivity where only convection is considered can be considered as convenient—the charged nonconducting structures could be considered as 'dielectric'. We thus studied possibility of creation of such structures in the regions where the jets should be created by the Blandford-Znajek process, i.e., near the symmetry axis of the magnetized black hole.

In modeling jets created by the Blandford-Znajek process, the assumed magnetic field has the character of the split magnetic monopole or some kind of parabolic field. In the present paper we concentrated attention on the case of the split magnetic monopole because this kind of magnetic field can be considered in vicinity of the black hole event horizon as an appropriate approximation of the magnetic fields created by a charged loop orbiting in the equatorial plane of the central black hole [20,21,34].

We have demonstrated the existence of nonconducting charged tori located off the equatorial plane for properly chosen parameters governing their location and structure; namely, the distribution of the specific angular momentum, and the electric charge density. Existence of such off-equatorial charged tori was proven for the profiles with $\ell = \text{const.}$ and $\Omega = \ell^2/K$. On the other hand, we have shown that charged tori with uniform rotation (with $\Omega = \text{const.}$) are not allowed. We have given detailed study of the possible center positions and shape of the off-equatorial charge tori.

We conclude that we were able to demonstrate clearly existence of nonconducting charged tori created by heavy particles located off the equatorial plane that could be, under properly chosen condition on the charged matter, its distribution, and distribution of the specific angular momentum governing their equilibrium configurations, allowed to occur near the symmetry axis of the magnetized black hole. The charged tori located near the symmetry axis could represent a possible obstacle for the matter of the jets that should probably interact with such configurations—the accelerated electrons should collide with heavy particles constituting the charged tori. Interactions of extremely accelerated electrons of the jet with the equilibrium tori created by heavy particles should lead to specific effects that could be observed, and maybe to some modifications of the Blandford-Znajek process. Clearly, the phenomenon of charged nonconducting tori located near the symmetry axis would be a serious challenge for future research in the field of accretion disks and related jets.

ACKNOWLEDGMENTS

The authors acknowledge support of the Research Centre for Theoretical Physics and Astrophysics, Institute of Physics, Silesian University in Opava. Z. S. acknowledges the Czech Science Foundation Grant No. 16-03564Y.

[1] M. A. Abramowicz and P. Ch. Fragile, Foundations of black hole accretion disk theory, Living Rev. Relativity **16**, 1 (2013).
[2] I. D. Novikov and K. S. Thorne, Astrophysics of black holes, in *Black Holes (Les Astres Occlus)*, edited by C. Dewitt and B. S. Dewitt (Gordon and Breach, New York, 1973), pp. 343–450.
[3] M. Kozlowski, M. Jaroszynski, and M. A. Abramowicz, The analytic theory of fluid disks orbiting the Kerr black hole, Astron. Astrophys. **63**, 209 (1978).
[4] Z. Stuchlík, P. Slaný, and S. Hledík, Equilibrium configurations of perfect fluid orbiting Schwarzschild-de Sitter black holes, Astron. Astrophys. **363**, 425 (2000).
[5] D. Pugliese and Z. Stuchlík, Ringed accretion disks: Equilibrium configurations, Astrophys. J. Suppl. Ser. **221**, 25 (2015).
[6] D. Pugliese and Z. Stuchlík, Ringed accretion disks: Instabilities, Astrophys. J. Suppl. Ser. **223**, 27 (2016).
[7] D. Pugliese and Z. Stuchlík, Ringed accretion disks: Evolution of double toroidal configurations, Astrophys. J. Suppl. Ser. **229**, 40 (2017).
[8] D. Pugliese and Z. Stuchlík, Relating Kerr SMBHs in active galactic nuclei to RADs configurations, Classical Quantum Gravity **35**, 185008 (2018).
[9] D. Pugliese and Z. Stuchlík, RADs energetics and constraints on emerging tori collisions around super-massive Kerr black holes, Eur. Phys. J. C **79**, 288 (2019).
[10] The internal, local magnetic fields are relevant due to the so-called magneto-rotational instability generating the disks viscosity causing accretion itself in Keplerian disks.
[11] M. Kološ, Z. Stuchlík, and A. Tursunov, Quasi-harmonic oscillatory motion of charged particles around a Schwarzschild black hole immersed in a uniform magnetic field, Classical Quantum Gravity **32**, 165009 (2015).
[12] Z. Stuchlík and M. Kološ, Acceleration of the charged particles due to chaotic scattering in the combined black

hole gravitational field and asymptotically uniform magnetic field, Eur. Phys. J. C **76**, 32 (2016).
[13] A. Tursunov, Z. Stuchlík, and M. Kološ, Circular orbits and related quasi-harmonic oscillatory motion of charged particles around weakly magnetized rotating black holes, Phys. Rev. D **93**, 084012 (2016).
[14] R. Pánis, M. Kološ, and Z. Stuchlík, Determination of chaotic behaviour in time series generated by charged particle motion around magnetized Schwarzschild black holes, Eur. Phys. J. C **79**, 479 (2019).
[15] Z. Stuchlík, M. Kološ, and A. Tursunov, Magnetized black holes: Ionized Keplerian disks and acceleration of ultra-high energy particles, Proceedings **17**, 13 (2019).
[16] J. Kovář, Z. Stuchlík, and V. Karas, Off-equatorial orbits in strong gravitational fields near compact objects, Classical Quantum Gravity **25**, 095011 (2008).
[17] J. Kovář, O. Kopáček, V. Karas, and Z. Stuchlík, Off-equatorial orbits in strong gravitational fields near compact objects—II: Halo motion around magnetic compact stars and magnetized black holes, Classical Quantum Gravity **27**, 135006 (2010).
[18] O. Kopáček, V. Karas, J. Kovář, and Z. Stuchlík, Transition from regular to chaotic circulation in magnetized coronae near compact objects, Astrophys. J. **722**, 1240 (2010).
[19] C. F. Gammie, J. C. McKinney, and G. Tóth, HARM: A numerical scheme for general relativistic magnetohydrodynamics, Astrophys. J. **589**, 444 (2003).
[20] S. S. Komissarov, Electrodynamics of black hole magnetospheres, Mon. Not. R. Astron. Soc. **350**, 427 (2004).
[21] R. D. Blandford and R. L. Znajek, Electromagnetic extraction of energy from Kerr black holes, Mon. Not. R. Astron. Soc. **179**, 433 (1977).
[22] N. Dadhich, A. Tursunov, B. Ahmedov, and Z. Stuchlík, The distinguishing signature of magnetic Penrose process, Mon. Not. R. Astron. Soc. **478**, L89 (2018).
[23] Z. Stuchlík, M. Kološ, J. Kovář, P. Slaný, and A. Tursunov, Influence of cosmic repulsion and magnetic fields on accretion disks rotating around Kerr black holes, Universe **6**, 26 (2020).
[24] J. Kovář, P. Slaný, Z. Stuchlík, V. Karas, C. Cremaschini, and J. C. Miller, Role of electric charge in shaping equilibrium configurations of fluid tori encircling black holes, Phys. Rev. D **84**, 084002 (2011).
[25] P. Slaný, J. Kovář, Z. Stuchlík, and V. Karas, Charged tori in spherical gravitational and dipolar magnetic fields, Astrophys. J. Suppl. Ser. **205**, 3 (2013).
[26] C. Cremaschini, J. Kovář, P. Slaný, Z. Stuchlík, and V. Karas, Kinetic theory of equilibrium axisymmetric collisionless plasmas in off-equatorial tori around compact objects, Astrophys. J. Suppl. Ser. **209**, 15 (2013).
[27] J. Kovář, P. Slaný, C. Cremaschini, Z. Stuchlík, V. Karas, and A. Trova, Electrically charged matter in rigid rotation around magnetized black hole, Phys. Rev. D **90**, 044029 (2014).
[28] J. Kovář, P. Slaný, C. Cremaschini, Z. Stuchlík, V. Karas, and A. Trova, Charged perfect fluid tori in strong central gravitational and dipolar magnetic fields, Phys. Rev. D **93**, 124055 (2016).
[29] A. Trova, K. Schroven, E. Hackmann, V. Karas, J. Kovář, and P. Slaný, Equilibrium configurations of a charged fluid around a Kerr black hole, Phys. Rev. D **97**, 104019 (2018).
[30] K. Schroven, A. Trova, E. Hackmann, and C. Lämmerzahl, Charged fluid structures around a rotating compact object with a magnetic dipole field, Phys. Rev. D **98**, 023017 (2018).
[31] J. Kovář, Y. Kojima, P. Slaný, Z. Stuchlík, and V. Karas, Charged fluids encircling compact objects: Force representations and conformal geometries, Classical Quantum Gravity **37**, 245007 (2020).
[32] R. M. Wald, Black hole in a uniform magnetic field, Phys. Rev. D **10**, 1680 (1974).
[33] A. Trova, V. Karas, P. Slaný, and J. Kovář, Electrically charged matter in permanent rotation around magnetized black holes: A toy model for self-gravitating fluid tori, Astrophys. J. Suppl. Ser. **226**, 12 (2016).
[34] S. S. Komissarov, Observations of the Blandford–Znajek process and the magnetohydrodynamic Penrose process in computer simulations of black hole magnetospheres, Mon. Not. R. Astron. Soc. **359**, 801 (2005).
[35] J. D. Jackson, *Classical Electrodynamics*, 3rd ed. (Wiley, New York, 1998).
[36] Of course, it would be instructive to consider both the terms in the right hand side of the Ohm's law, leading to much more complex configurations including the conducting electric flows and possible strong self-electromagnetic fields. We plan such studies in future research.
[37] J. D. Bekenstein and E. Oron, New conservation laws in general-relativistic magnetohydrodynamics, Phys. Rev. D **18**, 1809 (1978).
[38] M. Abramowicz, M. Jaroszynski, and M. Sikora, Relativistic, accreting disks, Astron. Astrophys. **63**, 221 (1978).
[39] Z. Stuchlík, Influence of the relict cosmological constant on accretion discs, Mod. Phys. Lett. A **20**, 561 (2005).
[40] Z. Stuchlík, P. Slaný, and J. Kovář, Pseudo-Newtonian and general relativistic barotropic tori in Schwarzschild-de Sitter spacetimes, Classical Quantum Gravity **26**, 215013 (2009).